International Journal of
High-Rise Buildings
www.ctbuh-korea.org/ijhrb/index.php

International Journal of High-Rise Buildings
December 2023, Vol 12, No 4, 335-341
https://doi.org/10.21022/IJHRB.2023.12.4.335

Experimental Study of Moisture-Wicking Fabric as Cooling Pad for Novel Rotary Direct Evaporative Cooler

Sang-Hwan Park and Jae-Weon Jeong†

Department of Architectural Engineering, Hanyang University, Korea

Abstract This study proposes a novel rotary direct evaporative cooler and investigates the potential of a moisture-wicking fabric as a cooling pad for the proposed evaporative cooler. The rotary direct evaporative cooler rotates the cooling pad to reduce the water and energy consumption of the pump compared to those of existing direct evaporative coolers. A moisture-wicking fabric is considered as the material of the cooling pad, because of its high moisture-wicking property, enhancing water evaporation. Experiments are performed under various inlet air conditions while measuring the air temperature, relative humidity, air velocity, and differential pressure. The evaporative cooling efficiency and impacts of the inlet air temperature and air velocity on the cooling performance are also evaluated. The results demonstrate the potential of the moisture-wicking fabric as cooling pad of direct evaporative cooler.

Keywords Direct evaporative cooler, Cooling efficiency, Moisture-wicking fabric, Cooling pad

†Corresponding author:
Jae-Weon Jeong
E-mail:
jjwarc@hanyang.ac.kr

1. Introduction

A direct evaporative cooler (DEC) is an evaporative cooling system in which air and water are in direct contact. Conventional DEC systems generally consist of a fan, pump, cooling pad, and water supply nozzle (Yang, 2019). The DEC sprays water to the porous cooling pad through the nozzle and passes air through the wetted pad. As the air passes through the wetted pad, water evaporates from the pad, and cools the air. DECs operate under a non-vapor compression method and do not use refrigerants. Therefore, DEC is a good alternative of heat pumps to reduce cooling energy consumption of building (Xuan et al., 2012). DEC is typically used to cool buildings or data centers in dry and hot climates.

Several studies have proposed integrating a DEC with an air conditioner to enhance the cooling performance of the air conditioner. In general, an air conditioner operates based on a vapor-compression cycle to transfer heat from indoors to outdoors. The vapor-compression cycle is reverse Carnot cycle, which absorbs heat from the indoors and releases it to outdoors through the circulating refrigerant. As the outdoor temperature increases, the temperature of the refrigerant must rise to transfer the absorbed heat to outdoors, resulting in the increased energy consumption of the compressor. Integrating a DEC with the air conditioner can reduce the energy consumption of the compressor. The temperature of refrigerant can be dropped by pre-cooling the outdoor air before the air enters the condenser. Hajidavalloo and Eghtedari (2010) compared a cooling system with a 5 cm thick cellulous media pad installed on the front of the condenser of a conventional split-air-conditioner with another conventional air conditioner. Results showed that the power consumption of air conditioner decreased by up to 20% and total performance improved by approximately 50%. Yang, H et al. (2021) experimentally investigated the integration of a spray DEC and air-cooled condenser. The results showed that the spray DEC enhanced the cooling performance of the air-cooled condenser by up to 42.6%. Kim et al. (2022) evaluated the energy saving potential of an air-source heat pump with a DEC using simulations. The results showed that the proposed operation strategy reduced energy consumption by 8.87%. Harby and Amri (2019) investigated the optimal thickness of the pad when using a DEC for pre-cooling a condenser. The experimental results showed that the optimal thickness was 100 mm, with energy consumption decreasing from 15% to 22% and the coefficient of performance (COP) increasing from 29% to 53%, depending on the ambient conditions. Comprehensively, the integration of the DEC and the air conditioner can effectively reduce energy consumption and improve the COP of the air conditioner.

New materials for cooling pads of DEC have been investigated to replace conventional commercial pads. Jain and Hindoliya (2011) tested the pads made of coconut

and palash fibers in a laboratory and compared them with the pads made of aspen and khus fibers. The experimental results showed that the cooling efficiency of the coconut fibers pad was 8.15% more than khus pad, and the cooling efficiency of the palash pad was 13.2% and 26.31% higher than aspen and khus pads, respectively. Gunhan et al. (2007) evaluated pumice stones, volcanic tuff, and greenhouse shading nets as alternatives of commercial "CELdek" pad. The experimental results showed that volcanic tuff pads can be alternatives of the "CELdek" pad at a 0.6 m/s air velocity. Liao and Chiu (2002) conducted wind tunnel experiments to evaluate the cooling performances of pads made of coarse fabric polyvinyl chloride (PVC) sponge with a 2.5 mm diameter pinhole and a fine fabric PVC sponge with a 7.5 mm diameter pinhole. The experimental results showed that the cooling efficiency varied from 81.75% to 84.48% and from 76.68% to 91.64% for the coarse and fine fabric, respectively. Eloy et al. (2020) investigated the potential of a cooling pad made of cotton fabric. The experimental results showed that the cooling efficiency varied from approximately 60% to 95%. Xu et al. (2016) investigated the wicking, diffusivity, and evaporation performance of six cloth fabrics and one Kraft paper. The results showed that two of six fabrics were suitable for indirect evaporative cooling applications.

From the above literature review, many studies have been performed for the integration of the DEC with air conditioner to enhance the cooling performance of the air conditioner and reduce energy consumption. Moreover, aiming to replace existing cooling pads, the cooling performances of cooling pads with various new materials have been investigated. However, conventional DECs continuously operates water supply pump to achieve uniform wettability of the cooling pads to maintain evaporative cooling performance, resulting in excessive pump energy and water consumption. In this study, a novel rotary DEC (RDEC) is proposed to reduce the excessive energy and water consumption of conventional DECs and the potential of moisture-wicking fabric, especially Coolmax, as a cooling pad of the proposed RDEC is investigated. In addition, the impacts of the operating conditions (air velocity, inlet air temperature) on the cooling performance of the cooling pad using the proposed moisture-wicking fabric (air temperature drop, relative humidity change, cooling efficiency, and differential pressure) are evaluated.

2. System Overview

2.1. Rotary direct evaporative cooler

Figure 1. shows the structure of the RDEC proposed in this study. The RDEC consists of a motor, a belt-pulley, rotation pipe, cooling pad, support pipes, and water sump. The motor, belt-pulley, rotation pipe, and cooling pad are connected for rotational movement and pipes support the cooling pad. Conventional commercial cellulose pads cannot

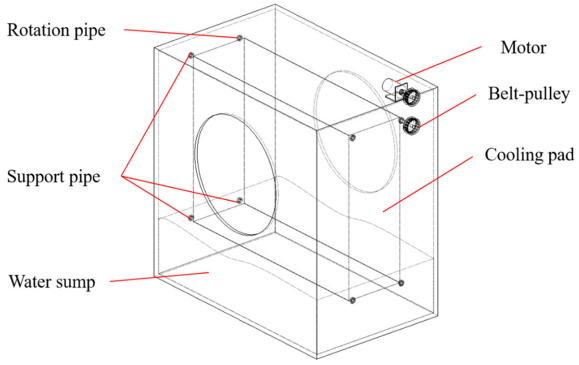


Figure 1. Structure of rotary direct evaporative cooler.

be used in the proposed RDEC due to their rigid structures. Therefore, a moisture-wicking fabric with a high evaporation performance, is considered as the material for the cooling pad of the RDEC.

The RDEC operates as follows. The cooling pad made of moisture-wicking fabric rotates at a constant speed. As the pad rotates, the dry surface of the pad moves into the water sump at the bottom of the RDEC and becomes wet. Next, the wet surface of the pad rises and contacts with the hot inlet airflow, which passes through the wet surface of the pad. Water evaporates from the pad and the airflow is cooled. This process is repeated as the pad continues to rotate. Excessive water spray for uniform wettability will be prevented and as the water pump operates only when the amount of the water in the sump below a certain level, water and pump energy consumpton can be reduced compared to conventional DEC.

2.2. Moisture-wicking fabric

A moisture-wicking fabric absorbs moisture and transports it to the outer surface of the fabric, enhancing evaporation of water. In this study, Coolmax is used as an example of a moisture-wicking fabric. Coolmax consists of polyester fibers and is designed to enhance the evaporation of sweat from the skin(Wang, 2008, Xu, 2021). The polyester fibers of Coolmax have an elliptical cross-section with fine grooves on the surface. These grooves form capillary channels enabling the transport of moisture. The moisture-wicking property of Coolmax is attributed to the capillary force from the grooves and hydrophobicity of the polyester. In the Coolmax fiber, the capillary action is driven by the adhesion force between the water and polyester, which is stronger than the cohesion force between the water molecules. This capillary action causes the water to move along the grooves of the fibers and results in the uniform wettability of the fabric. Moreover, the hydrophobicity of the polyester fibers prevents water from being absorbed into the fibers and enhances evaporation. Comprehensively, a continuous flow of moisture proceeds to the outer surface of the Coolmax fabric because of the moisture-wicking property, resulting in enhanced evaporation performance due to the increased air-water contact area.

3. Experimental Method

3.1. Experimental setup

An experimental setup was designed to investigate the cooling performance of the Coolmax fabric as cooling pad of proposed RDEC under various inlet air condition. The experimental device consists of a climate chamber, blower, and evaporative cooling device and Cooling pad made of Coolmax fabric. The size of the experimental device was a 300 mm (width) × 300 mm (height) × 500 mm (length) acrylic box. The inside of the device was finished with silicone to minimize air leakage during the experiment, and the insulation was attached to the outside surface of the device to minimize heat transfer to the surroundings. Thin acrylic bars were installed on the inside surface of the device to fix the Coolmax pad. The cooling pad consists of Coolmax fabric and center-holed acryl plate and the size was 300 mm (width) × 300 mm (height). Coolmax fabric was supported by a center-holed acrylic plate. The blower was controlled by a voltage controller to control the inlet air velocity. Figure 2. shows the experimental setup. The evaporative cooling device, blower, and climate chamber were linearly connected by the circular duct and duct connector flange. The diameter of both the duct and flange was 150 mm. The measuring instruments were a data logger, digital humidity / temperature probes, a vane probe, and a digital pressure manometer. The parameters, ranges, accuracies and resolutions of the measuring instruments are indicated in Table 1.

Initially, the conditioned air from the chamber entered to the evaporative cooling device by the controlled blower. The pad is completely wetted by tap water and installed in the evaporative cooling device when the inlet and outlet air condition of the device was equal. The entered air passed through the cooling pad, causing evaporation. Because of the evaporation, the sensible heat of the air changes to the latent heat of the water vapor. As the water evaporates from the pad, the pad gradually dried. The experiment ended when the pad was completely dry and the outlet air temperature was close to inlet air temperature. The digital humidity / temperature probes were located at the inlet and outlet of the evaporative cooling device and the vane probe was located at the



Figure 2. Experimental setup: (a) Experimental device, (b) Evaporative cooling device and cooling pad.

Table 1. Specifications of measuring instruments

Measuring instruments	Parameter	Range	Accuracy	Resolution
Testo 605i (inlet, outlet)	Temperature, Relative humidity	–20°C – 60°C, 0~100%	± 0.5°C (0~60 °C) ± 1.8% RH + 3% of measured value (5~80% RH)	± 0.1°C, ± 0.1%
Testo vane probe	Air velocity	0.3~35 m/s	± (0.1 m/s + 1.5% of measured value) (0.3~20 m/s) ± (0.2 m/s + 1.5% of measured value) (20~35 m/s)	± 0.01 m/s
Testo 510i	Pressure drop	± 150 hPa	± 0.05 hPa (0~1 hPa)	0.01 hPa

outlet of the device and the digital pressure manometer was connected to the inlet and outlet ducts of the device.

3.2. Evaporative cooling efficiency

In the direct evaporative cooling process, the theoretical limit of cooling temperature is the wet bulb tem-perature of inlet air. The cooling efficiency of the evaporative cooling (η) is expressed according to the inlet air temperature (T_i), outlet air temperature (T_o), and wet bulb temperature of the inlet air ($T_{wb,i}$) as follows: (Eq.(1)) (Carmargo, 2005)

$$\eta = \frac{T_i - T_o}{T_i - T_{wb,i}} \tag{1}$$

3.3. Experimental procedure

The experiment was conducted under two different scenarios: varying inlet air temperature and air velocity. The experimental conditions and procedures were as follows.

Scenario 1: Varying the inlet air temperature. The inlet air temperature was set to 30, 32, 33, 36, and 37°C, respectively. The air velocity was fixed at 1 m/s.

Scenario 2: Varying the air velocity. The air velocity was set to 1, 1.5, 2, and 2.5 m/s, respectively. The inlet air temperature was fixed at 36°C.

The temperature and humidity conditions of the inlet and outlet were maintained by the constant temperature and humidity chamber and the inlet and the outlet air conditions were initially set equally. The tap water temperature for wetting the pad was 20°C during the experiment. For a stable evaporative cooling performance, two cooling pads were overlapped and completely wetted with water and installed in the evaporative cooling device. Each experiment was finished when the evaporative cooling was completed, and the temperatures of the inlet and outlet reached equal again.

3.4. Uncertainty analysis

In this study, an uncertainty analysis was performed on the experimental data using the propagation of error method. In the propagation of error method, the uncertainty of a function f(x_1, x_2, ..., x_n) can be calculated as follows:

Table 2. Uncertainty analysis

Parameter	Minimum	Maximum
Wet bulb temperature ($T_{wb,i}$)	± 0.81°C	± 0.87°C
Cooling efficiency (η)	± 8.7%	± 18.2%

(Eq.(2)) (Moffat, 1988)

$$\mu_f = \sqrt{\sum_{i=1}^{n} \left(\frac{\partial_f}{\partial_{x_i}} u_{x_i} \right)^2} \tag{2}$$

In the Eq.(2), u_{x_i} is the uncertainty of the input variable x_i. The uncertainty of the evaporative cooling efficiency is calculated using Eq.(1) and (2). In this study, the uncertainty of wet bulb temperature was calculated based on the uncertainty of measured air temperature and relative humidity and the wet bulb function of the Engineering Equation Solver commercial version 10.836-3D. The uncertainty of the calculated parameters is shown in Table 2. The uncertainty of wet bulb temperature is from ± 0.81°C to ± 0.87°C, that of cooling efficiency is from ± 8.7% to ± 18.2%. The high uncertainty value of the cooling efficiency is because of the propagation from the high accuracy ranges of the measuring instruments.

4. Results and Discussion

The obtained results show that the evaporative cooling performance of the cooling pad made of Coolmax is sufficient for the direct evaporative cooler. The effect of the inlet air temperature on the evaporative cooling efficiency of the cooling pad is insignificant. As the air velocity increases, and as the pad contains more water, the differential pressure between the inlet and outlet increases because the resistance of pad to air increases. Therefore, the water containment of the cooling pad should be properly maintained to maximize the evaporative cooling performance and reduce differential pressure.

4.1. Cooling performance of cooling pad

Table 3 and Table 4 show the experimental results for the evaporative cooling performance of the cooling pad made of Coolmax. The values are the average of each

Table 3. Air inlet and outlet conditions for various air velocities

Air velocity							
1 m/s		1.5 m/s		2 m/s		2.5 m/s	
Inlet	Outlet	Inlet	Outlet	Inlet	Outlet	Inlet	Outlet
35.6°C, 53.6%	28.2°C, 92.4%	35.7°C, 45.5%	25.9°C, 94.0%	35.3°C, 41.8%	25.6°C, 86.8%	36.6°C, 46.5%	27.5°C, 94.1%

Table 4. Air inlet and outlet conditions for various inlet air temperatures

Inlet air temperature									
30°C		32°C		33°C		36°C		37°C	
Inlet	Outlet	Inlet	Outlet	Inlet	Outlet	Inlet	Outlet	Inlet	Outlet
30.0°C, 66.4%	25.3°C, 97.6%	32.3°C, 49.1%	24.0°C, 92.8%	32.8°C, 53.8%	25.3°C, 93.6%	35.6°C, 53.6%	28.2°C, 92.4%	36.6°C, 57.9%	29.5°C, 93.3%

case. The results show that the pad effectively reduces the air temperature close to the wet bulb temperature of the inlet air, which is the theoretical limit of evaporative cooling, The relative humidity of the outlet air increases from at least from 86.8% to 94.1%.

4.1.1. Effect of air velocity

Figure 3. shows the evaporative cooling efficiency of the Coolmax pad for various air velocities. The cooling efficiency exceeded 90% for all the tested air velocities (1 m/s, 1.5 m/s, 2 m/s, 2.5 m/s). The air velocity did not significantly affect the evaporative cooling efficiency. However, the differential pressure across the pad increased with the air velocity. Figure 4. shows the linear relationship between the air velocity and differential pressure. The differential pressure was maintained at 54 Pa at an air velocity of 1 m/s and at 85.7 Pa at 2.5 m/s, respectively.

4.1.2. Effect of inlet air temperature

Figure 5. shows the outlet air temperature and relative humidity by evaporative cooling. The inlet air temperature and relative humidity range from 30°C to 37°C, and 49.1% to 66.4%, respectively, with the air velocity maintained at 1 m/s. The results shows that the outlet air was significantly cooled and almost saturated. Relative humidity. The air was cooled close to the wet bulb temperature at all inlet temperatures. Figure 6. shows the evaporative cooling efficiency of the Coolmax pad at various inlet air temperatures: 30°C, 32°C, 33°C, 36°C, and 37°C. For all cases, the air velocity was maintained at approximately 1 m/s and the differential pressure was approximately 50 Pa. The results show that the cooling efficiency is not significantly affected by the inlet air temperature. The cooling efficiency exceeded 90% for every case and did not increase with the inlet air temperature.

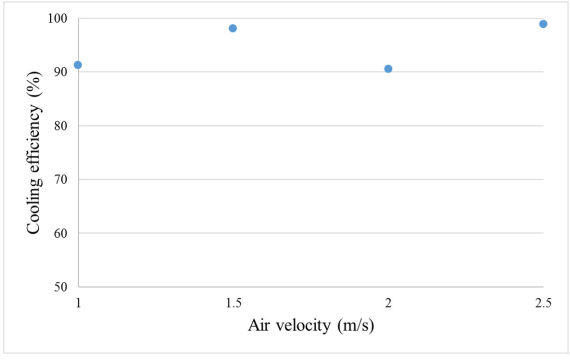


Figure 3. Cooling efficiency in various air velocities.

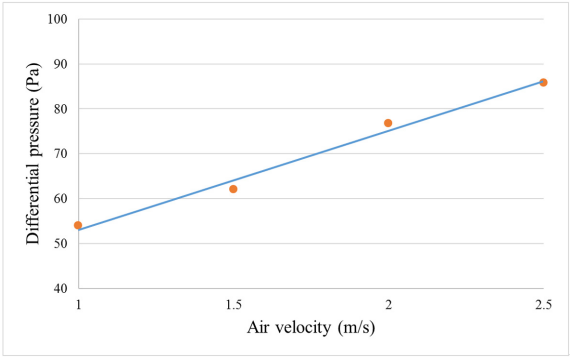


Figure 4. Differential pressure in various air velocities.

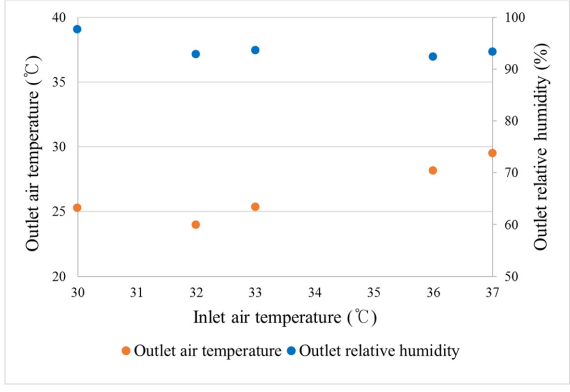


Figure 5. Outlet air temperature and relative humidity in various inlet air temperatures.

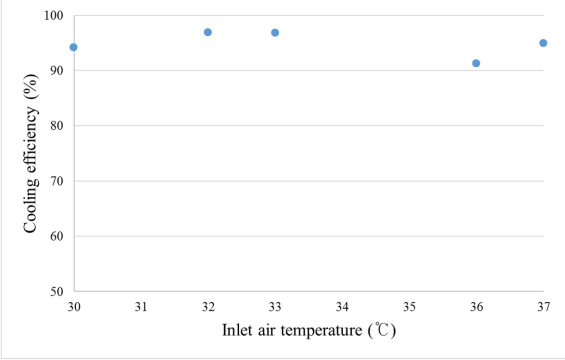


Figure 6. Cooling efficiency in various inlet air temperatures.

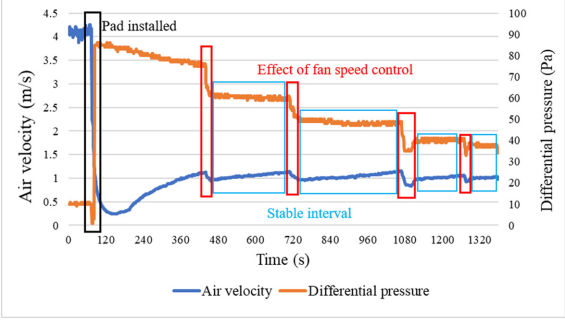


Figure 7. Transition of differential pressure over time.

4.2. Evaporative cooling performance of Coolmax

From Figure 3. and Figure 6, the evaporative cooling efficiency of Coolmax varied from 90.6% at 36°C and 2 m/s to 98% at 36°C and 1.5 m/s. The high evaporative cooling performance of Coolmax is attributed to the capillary force by unique grooved section and the hydrophobicity of polyester fibers of Coolmax, which enhances the evaporation of water.

4.3. Effect of water containment of cooling pad

Figure 7. shows the transient change of the air velocity and the differential pressure during experiment. shows the transient changes of the differential pressure over time. The inlet air temperature was 30°C and wet bulb temperature was 25°C. Before installing the pad, the differential pressure was approximately 10 Pa and the air velocity was 4 m/s. After installing the completely wet pad, the differential pressure increased to approximately 85 Pa and the air velocity decreased to approximately 0.3 m/s due to the resistance of the completely wet pad. The result shows that there is an optimal degree of water containment of the cooling pad to maintain proper air velocity with low differential pressure. Excessive water containment of the pad increases the differential pressure and reduces the air velocity.

5. Conclusions

This study proposes a novel RDEC, intending to reduce the excessive energy and water consumption of conventional DECs and the potential of using moisture-wicking fabrics, especially Coolmax, in the cooling pad of such RDECs was experimentally investigated. The evaporative cooling performance of the cooling pad was measured under various inlet air conditions. Based on experimental results, the cooling performances of the cooling pad were analyzed. The findings of this study are summarized as follows:

1. The evaporative cooling efficiency of the Coolmax pad ranges from 90.6% to 98%, which is impressive compared to the values of other materials. The effect of the inlet air temperature on the cooling efficiency was insignificant. The differential pressure increased with the air velocity from approximately 50 Pa at 1 m/s to approximately 90 Pa at 2.5 m/s.
2. Proper water containment of the cooling pads is important to optimize the performance of evaporative cooling systems. The increased resistance from the water in a completely wet pad leads to decreased air velocity and high differential pressure. After installing the cooling pad, the differential pressure increased from 10 Pa to 85 Pa and the air velocity decreased from 4 m/s to 0.3 m/s. Therefore, it is important to maintain adequate wettability of the cooling pad for proper cooling performance and avoid excessive pressure drop. The rotation speed of proposed RDEC is expected to be an important parameter to maintain adequate wettability of the cooling pad.

6. References

Yang, Y. et al. (2019). "Developments in evaporative cooling and enhanced evaporative cooling - A review." *Renewable and Sustainable Energy Reviews*, 113, 109230.

Xuan, Y. M. et al. (2012). "Research and application of evaporative cooling in China: A review (I) - Research." *Renewable and Sustainable Energy Reviews*, 16(5), 3535-3546.

Hajidavalloo, E. and Eghtedari, H. (2010). "Performance improvement of air-cooled refrigeration system by using evaporatively cooled air condenser." *International Journal of Refrigeration*, 33(5), 982-988.

Yang, H. et al. (2021). "Experimental study on an air-cooled air conditioning unit with spray evaporative cooling system." *International Journal of Refrigeration*, 131, 645-656.

Kim, B.-J. et al. (2022). "Energy performance enhancement in air-source heat pump with a direct evaporative cooler-applied condenser." *Case Studies in Thermal Engineering*, 35, 102137.

Harby, K. and Al-Amri, F. (2019). "An investigation on energy savings of a split air-conditioning using different commercial cooling pad thicknesses and climatic conditions." *Energy*, 182, 321-336.

Jain, J. K. and Hindoliya, D. A. (2011). "Experimental performance of new evaporative cooling pad materials."

Sustainable Cities and Society, 1(4), 252-256.

Gunhan, T. et al. (2007). "Evaluation of the Suitability of Some Local Materials as Cooling Pads." *Biosystems Engineering*, 96(3), 369-377.

Liao, C.-M. and Chiu, K.-H. (2002). "Wind tunnel modeling the system performance of alternative evaporative cooling pads in Taiwan region." *Building and Environment*, 37(2), 177-187.

Eloy, et al. "Experimental investigation of the potential of a new fabric-based evaporative cooling pad." *Sustainability*, 12.17 (2020), 7070.

Xu, P. et al. (2016). "Experimental investigation on performance of fabrics for indirect evaporative cooling applications." *Building and Environment*, 110, 104-114.

Wang, N. et al. (2008). "Study on the wicking property of polyester filament yarns." *Fibers and Polymers*, 9(1), 97-100.

Xu, L. et al. (2021). "Coolmax/graphene-oxide functionalized textile humidity sensor with ultrafast response for human activities monitoring." *Chemical Engineering Journal*, 412, 128639.

Camargo, J. R. et al. (2005). "Experimental performance of a direct evaporative cooler operating during summer in a Brazilian city." *International Journal of Refrigeration*, 28(7): 1124-1132.

Moffat, Robert J. (1988). "Describing the uncertainties in experimental results." *Experimental Thermal and Fluid Science*, 1.1, 3-17.